Synthesis, Characterization and Fabrication of Polyaniline and Polyaniline/Carbon Nanofiber on Indium Tin Oxide Glass by Dip Coating Technique

M. M. Rahman*[1], U.R. Ayan[1], M. Mim[1] and M. O. Faruk[2]

[1]*Department of Chemical Engineering and Polymer Science, Shahjalal University of Science and Technology, Sylhet, Bangladesh*
[2]*Department of Physics, Shahjalal University of Science and Technology*
Corresponding author: mrahman-cep@sust.edu

Received 26/11/2024; accepted 20/03/2025
https://doi.org/10.4152/pea.2027450104

Abstract
Polyaniline (PANI) is the oldest conducting polymer which has drawn demanding attention, due to its unique conductive properties and versatile applications in various fields. Carbon Nanofiber (CNF) is another promising material, due to its high electrical, thermal conductivity and great mechanical qualities, with various uses, including electrode constituents for batteries and supercapacitors (SC). The experiment of this study involved PANI and PANI/CNF synthesis, as well as the fabrication of their thin films on Indium Tin Oxide (ITO), using DCT. The primary focus was to examine electrical conductivity as a significant factor. The electrical conductivity of the hybrid composite consisting of PANI/CNF thin film-coated ITO was predominantly influenced by its dispersion state and thickness. Electrical conductance of PANI/CNF thin film on ITO glass prepared by Dip Coating Technique (DCT) was 41.78990 μS, whereas for PANI on ITO, and for bare ITO glass, was 7.30465 and 1.05238 μS, respectively. So, this study introduced a novel avenue for research in the domain of conducting polymers and their thin films on ITO substrates.

Keywords: CNF; conducting polymer; DCT; hybrid composites; ITO; PANI.

Introduction•

Synthesis and characterization of conductive polymers have garnered significant interest in the past twenty years [1-3], primarily due to their extensive potential for many applications, such as flexible electronics, thermoelectric devices, batteries, light-emitting diodes, electromagnetic shielding, SC and sensors [4, 5].
Electrically conducting polymers, such as PANI, polypyrrole (PPy) and polythiophene (PTh), have attracted considerable interest in scientific community,

•The abbreviations list is in pages 56-57.

owing to their remarkable chemical and electrochemical stability, with allows for easily preparation of large-area thin films, rendering them suitable for storing charge over their entire volume [6-9]. Moreover, these conductive polymers are favored over inorganic metal materials for fabrication of electronic products, due to their flexibility and compatibility with human skin, which requires dynamic, curved or elastic surfaces [10].

The future generation of soft and flexible electronics could be envisioned as consisting of conducting polymers, thus highlighting their potential to revolutionize electronic devices [11]. Moreover, recent research [12] has showcased thermoelectric characteristics of conductive polymers and revealed their low thermal conductivity and ability to adjust Seebeck coefficients via simple redox reactions, rendering them well-suited for thermoelectric applications [6-9].

An easy approach to enhance conductivity (by at least 5-fold) has been demonstrated by [13], through the stretching of an intrinsically conductive polymer - cyclic polyacetylene (PA) and polyvinyl chloride (PVC) - to 1.6 times its original length, simply by inducing molecular orientation. PA copolymerization with PVC has exhibited T-dependent conductivity. At least ten orders of magnitude in conductivity, correlating with the concentration of conjugated C-C double bonds and T, has been reported by [14]. Generation of new energy levels between conduction and valence bands, due to the inclusion of PPy in polyvinyl alcohol/chitosan composites, has been demonstrated by [15]. Referring to the study by [16], the ability to create an organized and extended π-conjugated system upon the inclusion of multiwalled carbon nanotubes in Pth backbone has significantly increased the conductivity of this composite.

Conductive polymers, especially PANI, have been particularly highlighted for their potential in SC applications, due to their high specific capacitance and favorable electrical properties [17]. It emerges as a highly promising conducting polymer, due to its easy polymerization process, exceptional chemical stability and comparatively elevated conductivity values [18]. PANI can be synthesized by chemical oxidative polymerization (COP), with inexpensive aniline and certain doping chemicals, resulting in a material with metal-like conductivity and electrochromic properties [19-21]. Technology exhibits a wide range of possible applications, including, but not limited to ECD and SC, which brings electromagnetic shielding effectiveness [22].

Incorporating graphene into PANI through doping significantly enhanced electrical conductivity [23]. Carbon black significantly enhanced electrical conductivity by establishing numerous conductive pathways within the polymer matrix [24]. Additionally, investigations into heterojunction composites made of NC from Au, PANI and TiO_2 have demonstrated improved photoelectrochemical biosensing performance, underscoring the contribution of titanium dioxide to composite materials enhancing [25].

As reported by [26], *in-situ* synthesis of reduced graphene oxide and PANI by emulsion polymerization has shown improved electrocatalytic activity, suggesting it as a promising cost-effective alternative for use as counter electrode. Furthermore, CNF is a nanometer-sized filament (from 3 to 100 nm in diameter) made up of stacked graphene layers that have a certain orientation with respect to the fiber axis. CNF and its composites have demonstrated significant potential in a variety of applications. The ability to tune their chemical and physical properties contributes to their versatility [27-28].

Nowadays, numerous investigations have been conducted thus far on transparent conductive film (TCF). Research has indicated that carbon nanotubes (CNT) thin films, ranging in thickness from 1 to 100 nm, have the potential to demonstrate both elevated electrical conductivity and notable optical transparency. Nevertheless, there exist certain obstacles that need to be overcome in order to enhance electrical conductivity and stability of CNT-based TCF [29]. To address this issue, CNF on TCF such as ITO glass substrates has been herein investigated. Several studies have suggested that the incorporation of cellulose nanofibers into a polymer matrix can lead to enhancements in both electrical conductivity and mechanical properties of resulting composite materials. As a result, there has been a recent surge of interest in NC comprised of CNF and conducting polymers. *In-situ* PANI/CNF composites have been synthesized by aniline via electrochemical oxidation. Due to PANI's strong affinity for the CNF surface, composites have potential uses in cells, sensors, micro/nano electronic components and optoelectronic devices with superior electrical, thermal or mechanical properties compared to PANI or CNF alone [22].

In this study, PANI and PANI/CNF were synthesized and subsequently fabricated into thin films on an ITO glass substrate using DCT. Electrical properties of these thin films, including conductance, capacitance, resistance and impedance, were thoroughly examined and analyzed. The primary goal of this study was to conduct a comparative analysis of electrical properties, specifically conductance, exhibited by two films that have been coated on ITO substrates. Additionally, the study aimed to determine which of the two films demonstrates superior conductivity.

Materials and methods

Materials

Aniline, $(NH_4)_2S_2O_8$, HCl (37%), acetone, ITO coated glass substrate (100 × 100 × 1.1 mm), within a thickness of about 188-190 nm, and ethanol were used as materials. Distilled water used in this experiment was produced in our laboratory. The compounds were of highest analytical purity.

Synthesis of PANI by COP

The synthesis was intentionally designed to be of utmost simplicity. Emeraldine salt of PANI was synthesized using COP process under acidic conditions, in which

aniline was present as cation. Various inorganic and organic acids of varying concentrations can be employed in PANI synthesis. In these instances, solubility, electrical conductivity and stability of resultant PANI vary depending on the acid used for protonation. In the current experimental study, HCl was chosen and employed in an equimolar ratio with aniline. $O_8S_2^{-2}$ ammonium salt was chosen over its potassium equivalent, due to its higher water solubility.

Literature allows for a wide range of oxidant/monomer ratios to be used. Stoichiometric aniline/$O_8S_2^{-2}$ ratio of 1.25 has been suggested for reducing the amount of residual aniline and maximizing PANI yield [30]. Since the oxidation of aniline is exothermic, T of the reaction mixture can be employed to track the reaction's progress [31-32].

Herein, 50 mL 2 M HCl were mixed in a beaker with 11.41 g $(NH_4)_2S_2O_8$, for 30 min, and vigorously stirred using a magnetic stirrer. In another beaker, 150 mL 2 M HCl were combined with 4.575 mL aniline. $(NH_4)_2S_2O_8$ was then added at 1 drop/2 sec to the acidic solution of aniline in an ice bath, for 4 h, to initiate polymerization reaction. The solution mixture was placed in the freezer after 4 h, where polymerization reaction persisted for the next 16 h. The resulting cake-like substance was then separated by filtration and dried for 24 h in a freeze dryer, to produce the desired product, Emeraldine salt of PANI.

Synthesis of PANI/CNF by COP

In this process, a PANI/CNF composite was made by polymerizing aniline as monomer in CNF presence. First, 4.60 mL aniline (monomer), 4.575 mL 2 M HCl and 0.050 g dried CNF suspension [15] were added to distilled water and stirred with a magnetic stirrer, until the solution was evenly mixed. The mixture was then put in an ice bath and mixed for 1 h, to cool it down to 0 ºC. To start polymerization, 11.41 g $(NH_4)_2S_2O_8$ dissolved in a 2 M HCl solution were slowly added to a blend of aniline and CNF, for 4 h. Then, the mixture was put in the freezer for 16 h, where polymerization process kept going. Then, a cake-like substance was made, which was filtered out and dried in a freeze-dryer to make a dark black powder.

Preparation of PANI thin film on ITO glass

In this work, a PANI thin layer was formed on ITO glass using DCT (Fig. 1).

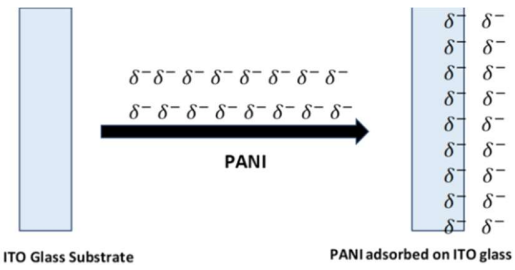

Figure 1: Schematic diagram of PANI film formation on ITO glass substrate.

The process of preparation was kept as basic as feasible. Polymerization of aniline in HCl was achieved by COP, followed by the formation of PANI thin film (likewise in PANI synthesis procedure). At the start of polymerization reaction, ITO glass substrate was immersed into the solution, for forming PANI thin film onto it. The reaction went for 4 h, after which freeze drying was done until a thin film of PANI was formed onto ITO glass substrate. Since aniline polymerization was exothermic, the experiment had to be carried out in an ice bath to minimize sudden heat release [33].

Preparation of PANI/CNF thin film on ITO glass substrate

PANI/CNF thin film on ITO glass (Fig. 2) was also synthesized under the same conditions followed by the same preparation method, as described in previous section. This specific amount of CNF was used as it was found that conductivity of PANI reached optimum value when 0.050 g CNF [33] was used in the synthesis process, and then started to decrease. Subsequent steps involved in the development of PANI/CNF thin film were identical to PANI thin film preparation method on ITO glass, as previously outlined.

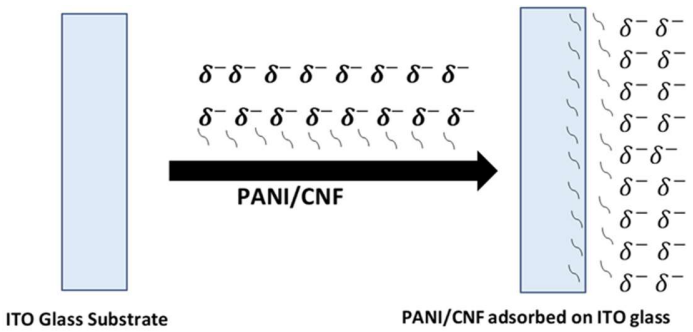

Figure 2: Schematic diagram of PANI/CNF film formation on ITO glass substrate.

Results and discussion

Characterization

For assessing electrical properties, PANI and PANI/CNF were synthesized, and their thin films on ITO glass were prepared by DCT, through polymerization reaction, followed by freeze drying in Biobase Freeze Dryer Bk-Fd10PT (tabletop type). For the powder sample, pellets were made from PANI and PANI/CNF powder samples using a hydraulic press machine with a 5×10^4 N load. The samples were then all labeled and kept in storage for testing. FTIR spectrums of synthesized samples, in the range from 500 to 4000 cm^{-1}, were recorded using FTIR spectroscopy (IRAffinity-1S). Determination of structural characteristics of PANI and PANI/CNF samples was carried out by XRD studies (RigakuSmartLab X-Ray diffractometer). Electrical properties of powder (PANI and PANI/CNF) and glass samples (bare ITO, PANI coated ITO and PANI/CNF coated ITO) were estimated by IA (Wayne kerr-6500B)

under 10 kHz frequency. Specific capacitance was evaluated by galvanostatic charge-discharge (GCD) analysis method by using Li-Po battery capacity analyzer (EBC-A20).

FTIR spectroscopy analysis

FTIR is an analytical method that uses infrared light to scan test samples and examine their chemical properties in order to identify organic, polymeric and inorganic compounds. The present study employed FTIR to investigate structural characteristics of both PANI and PANI/CNF NC. Fig. 3 depicts FTIR spectra of pure PANI and NC from PANI/CNF, respectively, throughout the frequency range from 4000 to 500 cm^{-1}.

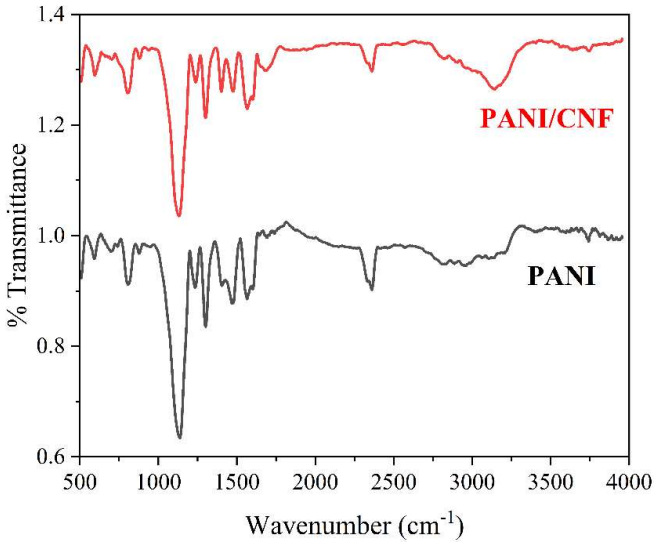

Figure 3: FTIR spectra of PANI and PANI-CNF.

Typical Pure PANI absorption bands were found at 1685.79, 1560.41, 1303.88, 1118.71, 1053.13 and 762 cm^{-1}. N-H stretching is represented by the typical peak at 3350.78 cm^{-1}. The broad band at 3200 cm^{-1} corresponds to the overlap of C-H stretching, benzenoid structural deformation and N-H bond stretching vibration. Emerald salt form of PANI was readily seen in this broad band. Characteristic peaks at 2968.44 and 1685.79 cm^{-1} are associated with PANI units' C-H and C-C stretching, respectively. Spectral peaks seen at wavenumbers 1560.41 and 1303.88 cm^{-1} correspond to the vibrational stretching of the aromatic ring, specifically, C-C-C bonds. Observed peaks corresponding to stretching vibrations of N-B-N and N-Q-N (where B represents benzoid and Q represents quinoid) are consistent with values published in existing scholarly literature. Peaks at a wavenumber of 1118.71 cm^{-1} can be assigned to C-N stretching vibration mode of N-Ph-N unit. Additionally, the peak observed at 762 cm^{-1} is indicative of a para-disubstituted aromatic ring, suggesting

the creation of a polymer [33]. Spectra of NC from PANI/CNF (Fig. 3) exhibit a high degree of similarity to those of pure PANI. The intensity of distinctive peaks observed in NC from PANI/CNF was found to be decreased in comparison to that of pure PANI. The presence of absorption bands in spectra provides unequivocal evidence of doped state from PANI. Aforementioned findings demonstrate both efficacy from PANI/CNF composite preparation technique and the absence of any detrimental impact on polymerization reaction from aniline to PANI in the presence of CNF [33].

XRD analysis

XRD is a technique used for microstructural research in order to determine polymer crystallinity, assess sample purity and investigate polymer orientation [34]. XRD patterns of pure PANI and PANI/CNF powder, as well as bare ITO, PANI and PANI/CNF thin films coated on ITO, were obtained within the range from 2θ = 5 to 80°. These patterns are depicted in Figs. 4 and 5.

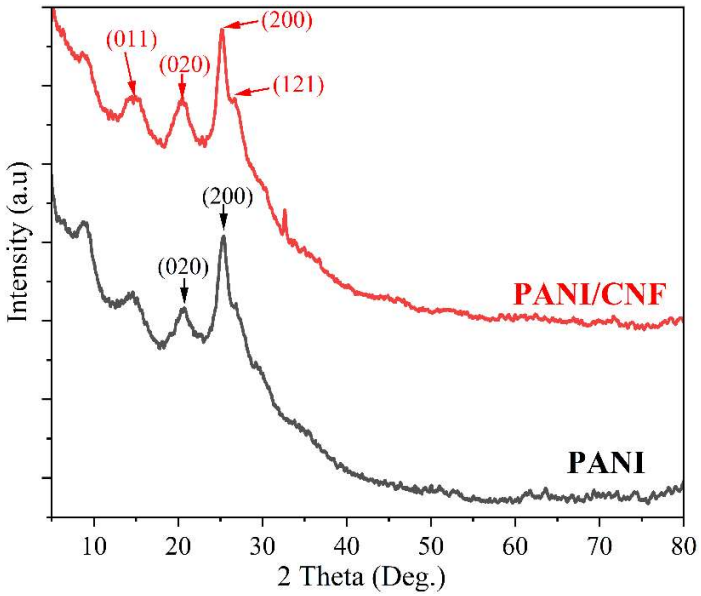

Figure 4: XRD patterns of PANI and PANI/CNF (powder).

A number of faint peaks with matching intensities were found, indicating that produced PANI and PANI/CNF powders are amorphous or semi-microcrystalline in nature [35]. Fig. 4 depicts a side-by-side XRD comparison between pure PANI and NC from PANI/CNF. The diffractogram shows that PANI was in an Emeraldine salt form, with peaks at 2θ = 20.5 and 25.4°, corresponding to (020) and (200) crystal planes, respectively. Repeated benzoid and quinoid rings in PANI chains are responsible for the compound's crystalline structure. The highest peak, which was

associated with the periodic array perpendicular to the polymer chain, revealing semi-crystalline structure of PANI, appeared at 2θ = 25.4°. The peak at 2θ = 20.5° was associated with periodic arrays parallel to the polymer chain. PANI production on the crystalline cellulose surface was demonstrated by the coexistence of distinctive peaks from PANI and CNF, at 16.1, 20.5, and 25.4 degrees in XRD of NC from PANI/CNF. By incorporating more CNF into the NC, the material crystallinity was improved [36].

Fig. 5 presents a comparison of XRD obtained from three samples: bare ITO glass, PANI coated ITO and ITO glass coated with PANI/CNF. The diffractogram obtained for both bare ITO and PANI coated ITO reveals the absence of distinct peaks, suggesting that both materials possess an amorphous or semi-microcrystalline structure. PANI/CNF coated ITO glass exhibits two distinct peaks at 2θ = 6.2 and 18.4°, suggesting an enhancement in its crystallinity, due to CNF incorporation.

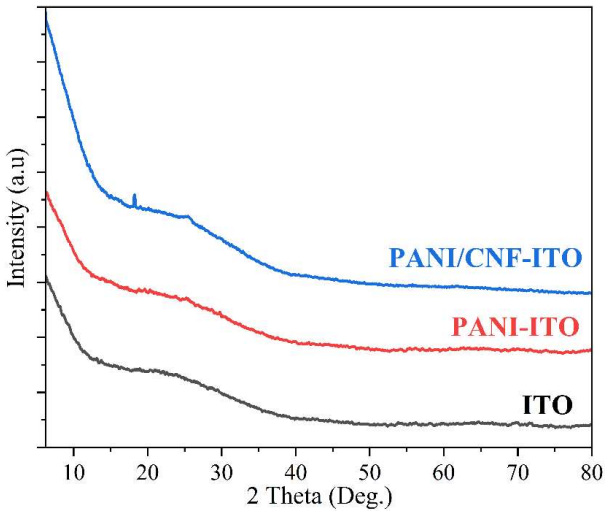

Figure 5: XRD patterns of bare ITO, PANI coated ITO and PANI/CNF coated ITO.

IA

Electrical parameters of the stored sample were measured using IA. An IA is a piece of electronic testing equipment that measures complex electrical impedance as a function of frequency. Most IA provide a reactance chart that displays capacitive (X_C) and inductive (X_L) reactance values for a given frequency. If any material tested by an IA is acting like a capacitor, the current flow through the material is restricted by internal impedance, which is known as capacitive reactance, usually denoted by X_c, which is inversely proportional to frequency. When frequency is very high, capacitive reactance (ohm) is usually very low. Results from IA are displayed in Table 1, which shows that conductance of PANI/CNF powder is higher than that from PANI. Other properties such as capacitance and loss factor were

greater for PANI/CNF powder, with less resistance, compared to PANI. Also, the table shows a 40-fold increase in conductance when PANI/CNF was coated on ITO, and a 7-fold increase in conductance when PANI was coated on ITO compared to that of bare ITO glass.

Table 1: Comparison of electrical parameter measurements of PANI and PANI/CNF powder, bare ITO glass, PANI coated ITO glass and PANI/CNF coated ITO glass.

Electrical parameters	PANI powder	PANI/CNF powder	Bare ITO glass	PANI coated ITO glass	PANI/CNF coated ITO
Conductance (μS)	28.0884	31.4932	1.05238	7.30465	41.78990
Resistance (kΩ)	35.6019	31.7529	171.262	136.899	23.9292
Capacitance (pF)	601.053	940.219	8.9238	378.085	5903.7
Loss factor	1.5391	1.7399	0.09618	3.25214	8.16031

In comparison to pure PANI, PANI/CNF composites exhibit enhanced conductivity, due to electron donor-acceptor interaction occurring between CNF and PANI components. CNF exhibits a higher electron-accepting nature in comparison to PANI, which demonstrates stronger electron-donating behavior. Coating of PANI with CNF promotes π–π* interaction between quinoid rings of PANI and CNF surface. In comparison to PANI coated ITO, PANI/CNF coated ITO has also less resistivity, high capacitance and high loss factor, which indicates that PANI/CNF coated ITO is a better electrically conductive material. Frequency *vs.* conductance of PANI/CNF coated ITO is shown in Fig. 6.

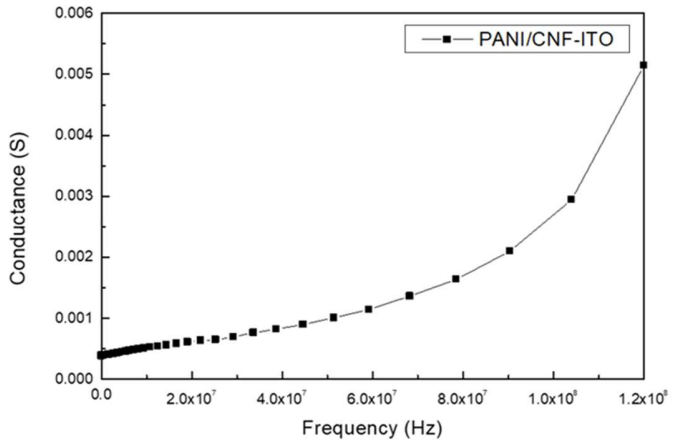

Figure 6: PANI/CNF coated ITO at different frequency range and conductance as function of frequency.

With change in frequency, its conductance continually increases. Results coming from conductance *vs.* frequency curve analysis indicate that PANI/CNF film coated ITO is a better conductive material. This conductive property of PANI/CNF film

coated on ITO can ensure its feasibility to be employed as electrode materials in solar cells, ECD and SC, as well as in electromagnetic shielding effectiveness.

GCD analysis

GCD analysis serves as valuable approach to evaluate specific capacity, while maintaining controlled current settings. C_{sp} was determined by employing discharge curves with eq. (1).

$$C_{sp} = I \times \Delta t \, \Delta V \times m \qquad (1)$$

where the variable "I" represents the applied current, "Δt" denotes CD discharge time, "ΔV" indicates potential and " m" represents average mass of active material present in the electrode [37].

Data coming from GCD analysis of PANI and PANI/CNF powder samples are presented in Table 2 with their respective curves (Figs. 7 and 8):

Table 2: Variation in specific capacitance, energy density and power density of PANI and PANI/CNF at different cycles.

Sample name	Properties	Cycle 1	Cycle 2	Cycle 3	Cycle 4	Cycle 5
PANI	Specific capacitance (F/g)	105.01	67.39	51.58	49.86	45.32
	Energy density (Wh/Kg)	7.94	5.68	3.78	3.91	3.23
	Power density (W/kg)	922.46	973.75	907	940	896
PANI/CNF	Specific capacitance (F/g)	147.7	66.37	49.6	43.8	39.68
	Energy density (Wh/Kg)	14.17	5.76	3.93	3.34	2.64
	Power density (W/kg)	1041.25	988.75	945	927.5	866.25

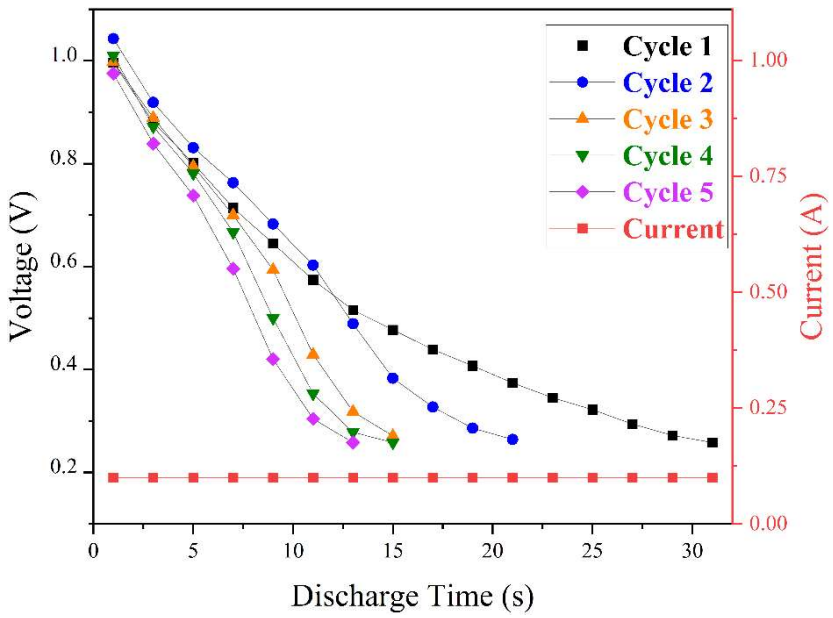

Figure 7: Variation of voltages at different cycles of PANI while discharging.

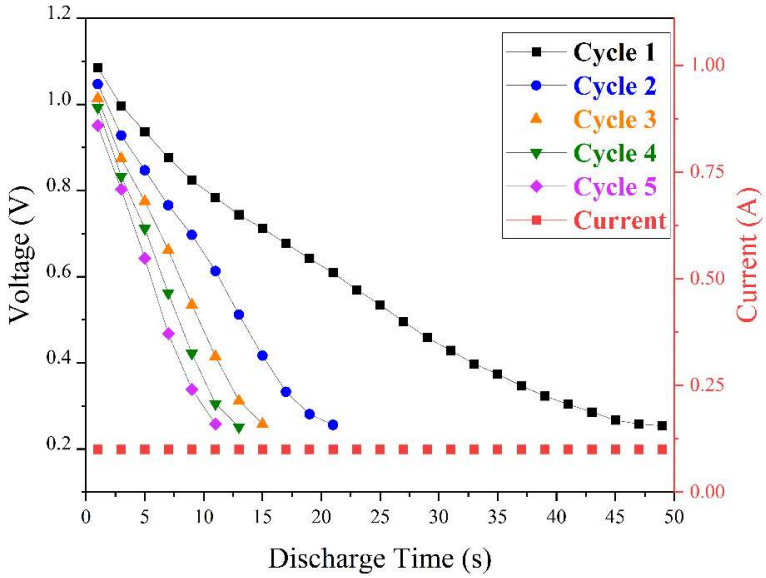

Figure 8: Variation of voltages at different cycle of PANI/CNF while discharging.

From Table 2 and their corresponding graph (Fig. 9), it can be noticed that specific capacitance from PANI/CNF composite material exhibits a significantly greater value than that from pure PANI in the 1st cycle (147.7 F/g). However, after the 5th cycle, PANI and PANI/CNF shows almost the same cyclic retention. Other properties such as energy density and power density of PANI/CNF are higher than that from PANI in cycle 1. Thus, it can be said that CNF increased PANI's properties without decreasing its cyclic retention. PANI/CNF shows higher specific capacitance than that from PANI.

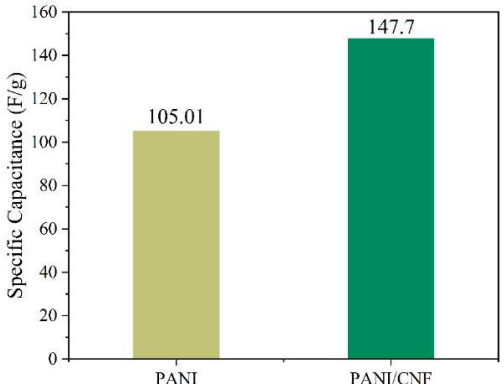

Figure 9: C_{sp} of PANI and PANI/CNF at cycle 1.

Conclusions

To conclude, according to results from IA, PANI/CNF thin film coated ITO hybrid composite generated by COP, followed by DCT, displayed greatly increased

electrical conductance (41.78990 μS) almost 40-fold higher than that from bare ITO glass. In comparison to pure PANI, PANI/CNF composite exhibits enhanced conductivity as a result of electron donor-acceptor interaction occurring between CNF and PANI components. Since the conductance of PANI-CNF coating can easily be manipulated by changing the film thickness on ITO glass substrate. Extensive research is needed, which will open a new window in this research area that will promote low-cost, easily scaled use of polymer-carbon composites in electrode applications.

Acknowledgement
The authors would like to acknowledge the financial support from SUST research center (Research grant 2020-2021, Project ID-AS/2020/1/21), Shahjalal University of Science and Technology, Sylhet, Bangladesh.

Conflict of interest
On behalf of all authors, the corresponding author states that there is no conflict of interest.

Authors' contributions
M. M. Rahman: conceptualization, supervision, writing – review and editing, funding acquisition, project administration. **U. R. Ayan**: synthesis, methodology, investigation, writing – original draft. **M. Mim**: synthesis, methodology, writing – original draft. **M. O. Faruk**: Impedance analysis.

Abbreviations
CNF: carbon nanofiber
COP: chemical oxidative polymerization
DCT: dip coating technique
ECD: electrochromic device
FTIR: Fourier-transform infrared
GCD: galvanostatic charge-discharge
HCl: hydrochloric acid
IA: impedance analyzer
ITO: indium tin oxide
$(NH_4)_2S_2O_8$: ammonium peroxydisulfate
NC: nanocomposite
$O_8S_2^{-2}$: peroxydisulfate
PANI: polyaniline
PPy: polypyrrole
Pth: polythiophene

SC: supercapacitor
T: temperature
TCF: transparent conductive film
XRD: X-ray diffraction

References

1. Mohd Y, Ibrahim R, Zainal MF. Electrodeposition and characterization of polyaniline films. IEEE Symp Human Sci Eng Res. 2012:1301-1306. https://doi.org/10.1109/SHUSER.2012.6268811
2. Wang Z, Cui H, Li S et al. Facile Approach to Conductive Polymer Microelectrodes for Flexible Electronics. ACS Appl Mater Interf. 2021;13(18):21661-21668. https://doi.org/10.1021/acsami.0c22519
3. Zhang Q, Sun Y, Xu W et al. Organic Thermoelectric Materials: Emerging Green Energy Materials Converting Heat to Electricity Directly and Efficiently. Adv Mat. 2014;26(40):6829-6851. https://doi.org/10.1002/adma.201305371
4. Yang Y, Deng H, Fu Q. Recent progress on PEDOT: PSS based polymer blends and composites for flexible electronics and thermoelectric devices. Mater Chem Front. 2020;4(11):3130-3152. https://doi.org/10.1039/D0QM00308E
5. Selvam J, Samannan B, Peter P et al. Synthesis, characterization, and solution studies of polyoxometalate-doped conducting polymers. Polym Polym Comp. 2021;29(5):373-382. https://doi.org/10.1177/0967391120918747
6. Abdulla HS, Abbo AI. Optical and electrical properties of thin films of polyaniline and polypyrrole. Int J Electrochem Sci. 2012;7(11):10666-10678. https://doi.org/10.1016/S1452-3981(23)16893-3
7. Grancarić AM, Jerkovic I, Koncar V et al. Conductive polymers for smart textile applications. J Industr Texti. 2018;48(3):612-642. https://doi.org/10.1177/1528083717699368
8. Lee KYT, Shi HH, Lian K et al. Flexible multiwalled carbon nanotubes/conductive polymer composite electrode for supercapacitor applications. Smart Mater Struct. 2015;24(11):115008. https://doi.org/0.1088/0964-1726/24/11/115008
9. Jain R, Tiwari DC, Karolia P. Electrocatalytic Detection and Quantification of Nitazoxanide Based on Graphene-Polyaniline (Grp-Pani) Nanocomposite Sensor. J Electrochem Soc. 2014;161(12):H839-H844. https://doi.org/10.1149/2.0911412jes
10. Chen X, He M, Zhang X et al. Metal-Free and Stretchable Conductive Hydrogels for High Transparent Conductive Film and Flexible Strain Sensor with High Sensitivity. Macromol Chem Phys. 2020;221(10):2000054. https://doi.org/10.1002/macp.202000054

11. Troughton J, Peillon N, Borbely A et al. High conductivity PEDOT: PSS through laser micro-annealing: mechanisms and application. J Mater Chem C Mater. 2022;10(43):16592-16603. https://doi.org/10.1039/D2TC03812A
12. Khan ZU, Edberg J, Hamedi M et al. Thermoelectric Polymers and their Elastic Aerogels. Adv Mat. 2016;28(22):4556-4562. https://doi.org/10.1002/adma.201505364
13. Shen Y-H, Yadav R, Wong AJ et al. Fibril size control, tensile strength, and electrical properties of cyclic polyacetylene. React Funct Polym. 2024;195:105810. https://doi.org/10.1016/j.reactfunctpolym.2023.105810
14. Rasmagin SI, Kryshtob VI. Electrical and Optical Properties of Polyvinyl Chloride–Polyacetylene Copolymer. Techn Physics. 2020;65(6):909-913. https://doi.org/10.1134/S1063784220060249
15. Elashmawi IS, Ismail AM, Abdelghany AM. The incorporation of polypyrrole (PPy) in CS/PVA composite films to enhance the structural, optical, and the electrical conductivity. Polym Bull. 2023;80(10):11379-11399. https://doi.org/10.1007/s00289-022-04611-6
16. Husain A, Ahmad S, Mohammad F. Electrical conductivity and ammonia sensing studies on polythiophene/MWCNTs nanocomposites. Materialia (Oxf). 2020;14:100868. https://doi.org/10.1016/j.mtla.2020.100868
17. Paul S, Kim JH, Kim DW. Cycling Performance of Supercapacitors Assembled with Polypyrrole/Multi-Walled Carbon Nanotube/Conductive Carbon Composite Electrodes. J Electrochem Sci Technol. 2011;2(2):91-96. https://doi.org/10.5229/JECST.2011.2.2.091
18. Huang LM, Chen CH, Wen TC et al. Effect of secondary dopants on electrochemical and spectroelectrochemical properties of polyaniline. Electrochim Acta. 2006;51(13):2756-2764. https://doi.org/10.1016/j.electacta.2005.08.012
19. Song E, Choi JW. Conducting Polyaniline Nanowire and its Applications in Chemiresistive Sensing. Nanomaterials. 2013;3(3):498-523. https://doi.org/10.3390/nano3030498
20. Liu W, Kumar J, Tripathy S et al. Enzymatically Synthesized Conducting Polyaniline. J Am Chem Soc. 1999;121(1):71-78. https://doi.org/10.1021/ja982270b
21. Liu W, Cholli AL, Nagarajan R et al. The Role of Template in the Enzymatic Synthesis of Conducting Polyaniline. J Am Chem Soc. 1999;121(49):11345-11355. https://doi.org/10.1021/ja9926156
22. Li XX, Zhao L, Ma D-Y et al. Polyaniline/carbon nanotube electrochromic films: Electrochemical polymerization and characterization. IOP Conf Ser: Mat Sci Eng. 2018;307(1):012068. https://doi.org/10.1088/1757-899X/307/1/012068

23. Rajyalakshmi T, Pasha A, Khasim S et al. Synthesis, characterization and Hall-effect studies of highly conductive polyaniline/graphene nanocomposites. SN Appl Sci. 2020;2(4):530. https://doi.org/10.1007/s42452-020-2349-4
24. Katheria A, Das P, Paul S et al. Preferential localization of conductive filler in ethylene-co-methyl acrylate/thermoplastic polyolefin polymer blends to reduce percolation threshold and enhanced electromagnetic radiation shielding over K band region. Polym Comp. 2023;44(3):1603-1616. https://doi.org/10.1002/pc.27191
25. Yan B, Zhao X, Chen D et al. Enhanced photoelectrochemical biosensing performance for Au nanoparticle–polyaniline–TiO_2 heterojunction composites. RSC Adv. 2020;10(72):43985-43993. https://doi.org/ 10.1039/D0RA06890J
26. Seema H, Zafar Z, Samreen A. Evaluation of solution processable polymer reduced graphene oxide transparent films as counter electrodes for dye-sensitized solar cells. Arab J Chem. 2020;13(4):4978-4986. https://doi.org/10.1016/j.arabjc.2020.01.020
27. Ruiz-Cornejo JC, Sebastián D, Lázaro MJ. Synthesis and applications of carbon nanofibers: a review. Rev Chem Eng. 2020;36(4):493-511. https://doi.org/10.1515/revce-2018-0021
28. Feng L, Xie N, Zhong J. Carbon nanofibers and their composites: a review of synthesizing, properties and applications. Materials. 2014;7(5):3919-3945. https://doi.org/10.3390/ma7053919
29. Zhou Y, Azumi R. Carbon nanotube based transparent conductive films: progress, challenges, and perspectives. Sci Technol Adv Mater. 2016;17(1):493-516. https://doi.org/10.1080/14686996.2016.1214526
30. Stejskal J, Gilbert RG. Polyaniline. Preparation of a conducting polymer (IUPAC technical report). Pure App Chem. 2002;74(5):857-867. https://doi.org/10.1351/pac200274050857
31. Sulimenko T, Stejskal J, Prokeš J. Poly (phenylenediamine) dispersions. J Colloi Interf Sci. 2001;236(2):328-334. https://doi.org/10.1006/jcis.2000.7415
32. Adams PN, Laughlin PJ, Monkman AP et al. Low temperature synthesis of high molecular weight polyaniline. Polymer (Guildf). 1996;37(15):3411-3417. https://doi.org/10.1016/0032-3861(96)88489-8
33. Rahman MM, Sarker DR, Faruk MO. Enhancement of Electrical Conductivity of Polyaniline Synthesized by using Carbon Nanofiber. J Sci Res. 2021;13(1):243-252. https://doi.org/10.3329/jsr.v13i1.48356
34. Inan TY. 2-Thermoplastic-based nanoblends: Preparation and characterizations. Micro and Nano Blends. Elsevier. 2017:17-56. https://doi.org/10.1016/B978-0-08-100408-1.00002-9
35. Devi MR, Saranya A, Pandiarajan J et al. Fabrication, spectral characterization, XRD and SEM studies on some organic acids doped polyaniline thin films on

glass substrate. J King Saud Univ Sci. 2019;31(4):1290-1296. https://doi.org/10.1016/j.jksus.2018.02.008

36. Razalli RL, Abdi MM, Tahir PM et al. Polyaniline-modified nanocellulose prepared from Semantan bamboo by chemical polymerization: preparation and characterization. RSC Adv. 2017;7(41):25191-25198. https://doi.org/10.1039/c7ra03379f
37. Abid MA, Radzi MI, Mupit M et al. Cyclic Voltammetry and Galvanostatic Charge-Discharge Analyses of Polyaniline/Graphene Oxide Nanocomposite based Supercapacitor. Malays J Comp Sci Manuf. 2020;3(1):14-26. https://doi.org/10.37934/mjcsm.3.1.1426